Dynamics of Concentrated Weakly Charged Polyelectrolyte Solutions

Andrea Siciliano and Angelo Perico*

Istituto di Studi Chimico-Fisici di Macromolecole Sintetiche e Naturali, National Research Council, Via De Marini 6, 16149 Genova, Italy

Received September 7, 1995; Revised Manuscript Received December 14, 1995[⊗]

ABSTRACT: The static and dynamic structure factors of weakly charged polyelectrolytes in concentrated solutions are derived in the random phase approximation. The effects of polymer stiffness, excluded volume, charge fraction, and salt concentration are obtained and compared with the small angle neutron scattering experiments on poly(acrylic acid) gels. An accurate description of the short range interactions in the unperturbed polymer chain together with consideration of a moderate excluded volume effect is required to approximate the complicated experimental behavior.

Introduction

The dynamical properties of weakly charged polyelectrolytes in concentrated solutions are expected to depend strongly on the conformational details of the chain, the charge fraction of monomers, and the ionic strength. The fluctuations of the concentration of the different species are coupled by electrostatic interactions, therefore influencing also the static and dynamic structure factors of the polymers.

The dynamics of flexible highly concentrated polymers under the influence of the excluded volume interaction in nondraining conditions are well described by the Doi−Edwards theory in the random phase approximation[1] (RPA). Solving the resulting linearized Langevin equation for the collective coordinates, the Fourier transform components of the segment concentration, the static and dynamic structure factors are easily derived. This approach was recently extended by us[2] (paper I hereafter) to include partial draining effects and nonideally flexible chains. The dynamic structure factor of semiflexible polymers in concentrated solutions was derived, and it was found strongly affected by stiffness.

Ajdari et al.[3] extended the Doi−Edwards Langevin dynamics of the collective coordinates to weakly charged polyelectrolyte solutions considering coupled fluctuations of the three species: polymer segments, counterions, and salt ions. The starting point is the free energy for the concentration fluctuations of the three species, written according to Borue and Erukhimovich[4] as a quadratic form in the collective coordinates which takes into account excluded volume interactions, translational entropy of counterions and salt ions, and electrostatic interaction between the charge densities. In this paper, several improvements to this theory are introduced; semiflexible polymers and partial draining contributions are considered, following paper I, while the dynamic structure factor is exactly calculated avoiding approximations in the solution of the linearized Langevin equation.

Recent small angle neutron scattering (SANS) experiments on poly(acrylic acid) (PAA) gels[5,6] have shown remarkable effects: A maximum emerges in the wave vector dependence of the polymer static structure factor, associated with the emerging of a mesophase order in the solution, whose value and position decrease with ionic strength. This behavior is grossly explained by RPA models of concentrated solutions in poor solvents of weakly charged polyelectrolytes.[4,7] On the contrary, for the experimental behavior of the cooperative diffusion coefficient as a function of polymer concentration, ionization strength, and salt concentration, only a qualitative agreement was found,[3,4,7] showing that the modeling of the dynamics of these gels deserves further attention.

As a first step in this program, our improved theory will be compared with static and dynamic SANS experiments to test the effects of stiffness and excluded volume. An attempt is also suggested to include in the theory the electrostatic contribution[8,9] to the polymer stiffness in the two limits of intrinsically stiff and flexible chains.[10] These improvements will help to better isolate the residual effects originated by the network structure of the gels.

Langevin Equation and Dynamic Structure Factor

Consider a concentrated solution of weakly charged polyelectrolytes. Each polyelectrolyte has n beads carrying fraction f of monovalent charges. The bead concentration in the solution is c_1, the concentration of monovalent counterions (of polyion and salt) is c_2, and the concentration of monovalent dissociated salt is c_3. The average charge density, $e\rho$, is zero due to the electroneutrality of the solution:

$$e\rho = e(fc_1 - c_2 + c_3) = 0 \tag{1}$$

The scattering experiments probe the local concentration fluctuations of the three species which in the Fourier space are represented as:

$$c_\alpha(\mathbf{k},t) = \frac{1}{V}\sum_{j=1}^{n_\alpha}\exp(-i\mathbf{k}\cdot\mathbf{R}_j(t)) \tag{2}$$

with n_1, n_2, and n_3 the number of polymer beads, counterions, and salt ions in the volume V. Describing the concentration by column vector $\mathbf{c}$ of components $c_\alpha(\mathbf{k})$, the static structure factor of the solution takes a 3 × 3 matrix form with components:

$$S_{\alpha\beta}(\mathbf{k}) = V\langle c_\alpha(\mathbf{k})c_\beta(-\mathbf{k})\rangle \tag{3}$$

The ensemble average of eq 3 is calculated using the equilibrium distribution function of the collective variable $c_\alpha(\mathbf{k})$. In the random phase approximation to the

[⊗] Abstract published in *Advance ACS Abstracts,* February 15, 1996.

0024-9297/96/2229-2068$12.00/0

unperturbed polymer distribution function and in the δ-function approximation to the excluded volume interactions between any two polymer beads in the concentrated solution,[1] the free energy describing all the concentration fluctuations is written as:[3,4]

$$F/k_BT = \frac{V}{2}\sum_{\mathbf{k}\neq 0}\Big\{((S_0(\mathbf{k}))^{-1} + \nu)c_1(\mathbf{k})c_1(-\mathbf{k}) + c_2^{-1}c_2(\mathbf{k})c_2(-\mathbf{k}) + c_3^{-1}c_3(\mathbf{k})c_3(-\mathbf{k}) + \frac{4\pi l_B}{k^2}\rho(\mathbf{k})\rho(-\mathbf{k})\Big\} \quad (4)$$

Here the first term in the right-hand side is the neutral polymer contribution with $S_0(\mathbf{k})$ the unperturbed polymer structure factor and ν the excluded volume parameter. The second and third terms are due to the translational entropy of the counterions and salt ions. The last term describes the electrostatic Coulombic interaction between all the charges in the solution, and

$$l_B = e^2/4\pi\epsilon k_BT \quad (5)$$

is the Bjerrum length with ϵ the dielectric constant and $\rho(\mathbf{k})$ the Fourier transform of the local charge density.

It is immediately recognized from eqs 3 and 4 that the free energy is a simple quadratic form in the variable $c_\alpha(\mathbf{k})$:

$$F/k_BT = \frac{V}{2}\sum_{\alpha,\beta}\sum_{\mathbf{k}\neq 0}\{(\mathbf{S}(\mathbf{k})^{-1})_{\alpha\beta}c_\alpha(\mathbf{k})c_\beta(-\mathbf{k})\} \quad (6)$$

The α,β element of the inverse of the static structure factor matrix $\mathbf{S}^{-1}$ is readily given as the second derivative with respect to the appropriate concentrations of the free energy (4):

$$S^{-1}{}_{\alpha\beta}(\mathbf{k}) = \frac{1}{V}\frac{\partial^2}{\partial c_\alpha(\mathbf{k})\partial c_\beta(-\mathbf{k})}(F/k_BT)$$

$$= \begin{bmatrix} S_0^{-1} + \nu + f^2\frac{4\pi l_B}{k^2} & -f\frac{4\pi l_B}{k^2} & f\frac{4\pi l_B}{k^2} \\ & c_2^{-1} + \frac{4\pi l_B}{k^2} & -\frac{4\pi l_B}{k^2} \\ & & c_3^{-1} + \frac{4\pi l_B}{k^2} \end{bmatrix} \quad (7)$$

In the element S_{11}^{-1}, the term $S_0^{-1} + \nu$ is the inverse of the static structure factor for a concentrated solution of neutral polymers with excluded volume ν in the random phase approximation, and S_0 is the unperturbed static structure factor for a single chain of n beads:

$$S_0(\mathbf{k}) = V\langle c_1(\mathbf{k})c_1(-\mathbf{k})\rangle_0 = c_1 n^{-1}\sum_{i,j}^{n}\exp\left(-\frac{k^2}{6}\langle|\mathbf{R}_i - \mathbf{R}_j|^2\rangle_0\right) \quad (8)$$

The excluded volume parameter is related to ξ_G, the correlation length of the concentration fluctuations for a perfectly flexible chain, through the relation:

$$\nu = l^2/12c_1\xi_G^2 \quad (9)$$

with l^2 the mean square segment length. The dynamic structure factor matrix is now derived starting from the linearized Langevin equation for the collective coordinate vector:[1,2]

$$\frac{\partial}{\partial t}c_\alpha(\mathbf{k},t) = -\frac{1}{V}\sum_\beta(k^2D_G)L_{\alpha\beta}(\mathbf{k})\frac{\partial}{\partial c_\beta(-\mathbf{k})}(F/k_BT) + r_\alpha(\mathbf{k},t) \quad (10)$$

with $L_{\alpha\beta}(\mathbf{k})$ the kinetic coefficients, in the preaveraging approximation, related to the random variables $r_\alpha(\mathbf{k},t)$ via the fluctuation−dissipation theorem

$$\langle r_\alpha(\mathbf{k},t)r^*{}_\beta(\mathbf{k},t)\rangle = \frac{2k^2D_G}{V}L_{\alpha\beta}(\mathbf{k})\delta(t - t') \quad (11)$$

Here

$$D_G = k_BT/6\pi\eta\xi_G \quad (12)$$

is the cooperative diffusion coefficient for a neutral flexible chain.[1]

The kinetic coefficients are calculated in the partial draining case following the Doi−Edwards procedure[1] extended, according to paper I, to include draining effects and non-Gaussian chains and taking into account all the components in the solution[3] as:

$$L_{\alpha\beta}(\mathbf{k}) = \frac{c_\alpha 6\pi\eta\xi_G}{\zeta_\alpha}\delta_{\alpha\beta} + \frac{6\pi\eta\xi_G}{4\pi^2\eta_0}\int_0^\infty dq\,\frac{h(q,k)}{k^2}[S_{\alpha\beta}(q) - S_{\alpha\alpha}(\infty)\delta_{\alpha\beta}] \quad (13)$$

with

$$h(q,k) = q^2\left[\frac{q^2 + k^2}{2qk}\ln\left|\frac{k+q}{k-q}\right| - 1\right] \quad (14)$$

The subtraction of $\delta_{\alpha\beta}S_{\alpha\alpha}(\infty)$ in eq 13 takes into account that the hydrodynamic interaction is effective only between different segments, a condition ignored in the nondraining approximation, and in addition ensures the convergence of the q integral.[2]

Substitution of eqs 13 and 4 in eq 10 finally gives

$$\frac{\partial}{\partial t}c_\alpha(\mathbf{k},t) = -k^2D_G\sum_\beta F_{\alpha\beta}(\mathbf{k})c_\beta(\mathbf{k},t) + r_\alpha(\mathbf{k},t) \quad (15)$$

The dimensionless rate constant matrix, defined as $\mathbf{F} = \mathbf{L}\mathbf{S}^{-1}$ has the elements $F_{\alpha\beta}$ given as:

$$F_{\alpha\beta} = c_\alpha\left(\frac{6\pi\eta\xi_G}{\zeta_\alpha}\right)(S^{-1}(k)_{\alpha\beta}) + \frac{3\xi_G}{2\pi}\sum_\gamma\left\{\int_0^\infty dq\,\frac{h(q,k)}{k^2}[S_{\alpha\gamma}(q) - \delta_{\alpha\gamma}S_{\alpha\gamma}(\infty)]S^{-1}(k)_{\gamma\beta}\right\} \quad (16)$$

The Langevin eq 15 for the collective coordinates $c_\alpha(\mathbf{k},t)$ can be decoupled by the transformation:

$$c_\alpha(t) = \sum_j Q_{\alpha j}\xi_j(t) \quad (17)$$

with $\mathbf{Q}$ the matrix of the eigenvectors of $\mathbf{F}$

$$\mathbf{Q}^{-1}\mathbf{F}\mathbf{Q} = \Lambda \quad (18)$$

Here the dimensionless λ_a, diagonal elements of Λ, are the eigenvalues of $\mathbf{F}$, function of the wavevector k. In the limit $k \to 0$, $D_G\lambda_l(0)$ has the meaning of polymer

cooperative diffusion coefficient:

$$D_C = \lim_{k\to 0} D_G\lambda_1(k) = D_G\lambda_1(0) \tag{19}$$

Note that at the same time the transformations:

$$\mathbf{Q}^{-1}\mathbf{L}\mathbf{Q}^{-1T} = \mathbf{N} \tag{20}$$

and

$$\mathbf{Q}^{T}\mathbf{S}^{-1}\mathbf{Q} = \mathbf{M} \tag{21}$$

reduce $\mathbf{L}$ and $\mathbf{S}^{-1}$ to the diagonal forms $\mathbf{N}$ and $\mathbf{M}$ of diagonal elements ν_a and μ_a with

$$\lambda_a = \nu_a\mu_a \tag{22}$$

due to eq 18.

The Langevin equation for the normal mode a becomes

$$\frac{d}{dt}\xi_a(t) = -k^2D_G\lambda_a\xi_a(t) + \xi_a{}^R(t) \tag{23}$$

with

$$\langle\xi_a{}^R(t)\xi_b{}^{R*}(t')\rangle = \frac{2k^2D_G}{V}\nu_a\delta_{ab}\delta(t-t') \tag{24}$$

Finally the time correlation functions (TCFs) for the normal variables result,

$$\langle\xi_a(t)\xi_b(0)\rangle = \frac{1}{V}\mu_a{}^{-1}\delta_{ab}\exp(-k^2D_G\lambda_a t) \tag{25}$$

while the dynamics of the structure factor is given as

$$S_{\alpha\beta}(k,t) = \frac{1}{V}\sum_{a=1}^{3} Q_{\alpha a}Q_{\beta a}\mu_a{}^{-1}\exp(-k^2D_G\lambda_a t) \tag{26}$$

Two interesting approximations to the important first eigenvalue $\lambda_1(k)$, describing the relaxation of polymer concentration fluctuations (see below), are the element F_{11}:

$$F_{11} = c_1\left(\frac{6\pi\eta\xi_G}{\zeta_1}\right)(S^{-1}(k)_{11}) + \frac{3\xi_G}{2\pi}\sum_\gamma\left\{\int_0^\infty dq\,\frac{h(q,k)}{k^2}[S_{1\gamma}(q) - \delta_{1\gamma}S_{11}(\infty)]S^{-1}(k)_{\gamma 1}\right\} \tag{27}$$

and the Ajdari et al.[3] expression, extended here in order to include chain stiffness

$$\lambda_1{}^a(k) = \frac{3\xi_G}{2\pi k^2}\int dq\; h(k,q)\frac{S_{11}(q) - S_{11}(\infty)}{S_{11}(k)} \tag{28}$$

The latter approximation amounts to take into account only the nondraining limit and to estimate the matrix product in the second term in the right-hand side of eq 27 by a simple scalar ratio involving only the element S_{11}.

From eq 28 evaluated at $p = 0$ and with $S_0{}^{-1}(kl) \cong (kl)^2/12c_1$, the following analytic form for the cooperative diffusion coefficient is obtained[3] in the $k \to 0$ limit:

$$\lambda_1{}^a(0) = \frac{k_BT\alpha^2}{D_G 6\pi\eta\kappa}\left(1 + \frac{\kappa^2}{\alpha^2}\right)\left[\frac{\nu}{\nu' - \nu} + 2\frac{\kappa^2}{\alpha^2} + \frac{\kappa^4}{\alpha^4}\right]^{-1/2} \tag{29}$$

where

$$\alpha^4 = \left[\frac{\nu'}{\nu' - \nu}\right]r_0{}^{-4} \tag{30}$$

and r_0 is a typical distance defined as

$$r_0{}^{-2} = \left(\frac{48\pi l_B}{l^2}\right)^{1/2} f c_1{}^{1/2} \tag{31}$$

Here

$$\nu' = \nu + \frac{4\pi l_B f^2}{\kappa^2} \tag{32}$$

is the global excluded volume including also the electrostatic contribution, and κ^{-1} is the Debye screening length: $\kappa^{-1} = [(fc_1 + 2c_3)4\pi l_B]^{-1/2}$.

Static Structure Factor

By inversion of matrix $\mathbf{S}^{-1}$ of eq 7, the static structure factor is obtained. As discussed in paper I, the effect of the conformational details of the chain can be included by taking the proper choice for the equilibrium mean-square interbead distances appearing in the unperturbed static structure factor of eq 8. For semiflexible chains, we choose a freely rotating chain (FRC) model. In this case these distances are given exactly[11] by:

$$\langle|\mathbf{R}_i - \mathbf{R}_j|^2\rangle = l^2|i-j|\left\{\frac{1+p}{1-p} - \frac{2p}{|i-j|}\frac{1-p^{|i-j|}}{(1-p)^2}\right\} \tag{33}$$

with

$$p = -\cos(\theta) \tag{34}$$

the stiffness parameter, θ the valence angle, and

$$l_0 = l(1-p)^{-1} \tag{35}$$

the bare persistence length. In the limit $p \to 0$ and $p \to 1$, the Gaussian expression $l^2|i-j|$ and the rod expression $l^2|i-j|^2$ are respectively recovered. The inversion of $\mathbf{S}^{-1}$ gives for each term in $\mathbf{S}$ complicated dependences on the parameters characterizing the polyelectrolyte solution:

$$\mathbf{S} = [k^2(S_0{}^{-1}(k) + \nu) + \kappa^2(S_0{}^{-1}(k) + \nu')]^{-1} \times \begin{bmatrix} k^2+\kappa^2 & 4\pi l_B f c_2 & -4\pi l_B f c_3 \\ & c_2\{(S_0{}^{-1}(k)+\nu)(k^2+4\pi l_B c_3)+ & 4\pi l_B c_2 c_3(S_0{}^{-1}(k)+\nu) \\ & 4\pi l_B f^2\} & c_3\{(S_0{}^{-1}(k)+\nu)(k^2+4\pi l_B c_2)+ \\ & & 4\pi l_B f^2\} \end{bmatrix} \tag{36}$$

While one of the eigenvalues of $\mathbf{S}$ is found fairly well coincident with $S_{11}(k)$, the other two eigenvalues are practically polymer independent.

In Figure 1 the polymer contribution to the static structure factor, $S_{11}(k)$, is reported. For neutral solutions of flexible polymers, $S_{11}(k)$ takes its maximum value, $(S_0{}^{-1} + \nu)^{-1}$, at $k = 0$ and its minimum value, $c_1/(1 + c_1\nu)$, in the $k \to \infty$ limit. In the polyelectrolyte case, a maximum appears in the intermediate k range.

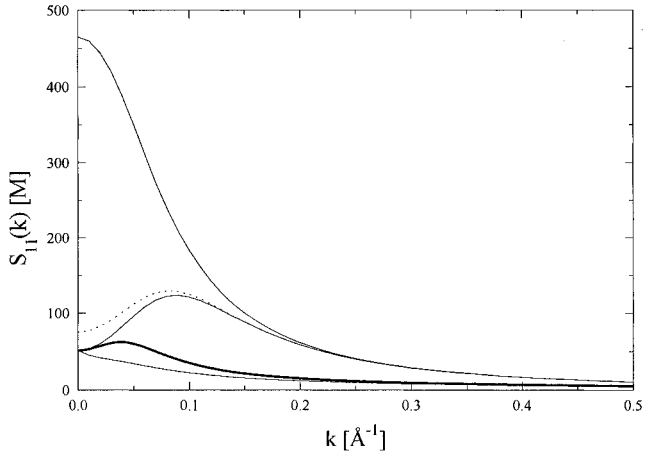

Figure 1. Polymer contribution to the static structure factor S_{11} at $l_b = 7$ Å, $l = 2.5$ Å, $c = 1.44$ M, $\nu = 1.45 \times 10^{-3}$ M^{-1}, and $n = 10^3$. From top to bottom: neutral polymer, $p = 0$; $f = 0.025$, $p = 0$; $f = 0.025$, $p = 0.8$; $f = 0.025$, rod limit. All the full curves have $c_3 = 0$ M. Dashed curve: $c_3 = 0.01$ M and $p = 0$.

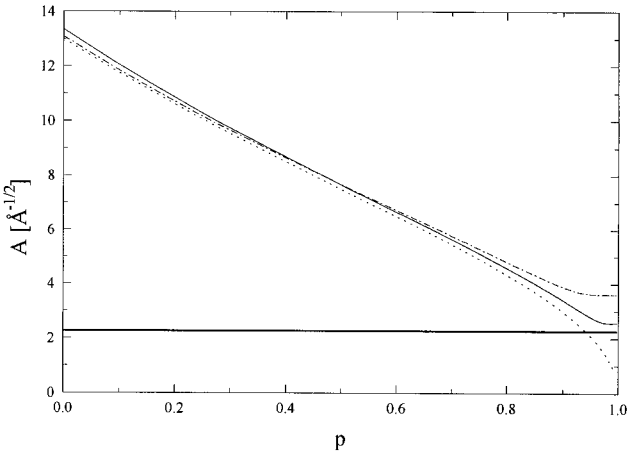

Figure 2. Quantity $A = [(k^*l)^2 + (\kappa l)^2]/fc_1^{1/2}l^2$ relative to the position of the maximum in $S_{11}(k)$ as a function of the polymer stiffness, p, in the reference state ($l_b = 7$ Å, $l = 2.5$ Å, $c_1 = 0.419$ M, $c_3 = 0$ M, $f = 0.025$, $\nu = 0$, $n = 10^3$): full curve. Dashed curve: $f = 0.025$. Dotted curve: eq 46 with a renormalized bond length, $l[(1 + p)/(1 - p)]^{1/2}$. The experimental result for PAA[5] is represented by the horizontal line.

The minimum at $k \rightarrow \infty$ remains the same, while the value in $k = 0$ becomes

$$S_{11}(0) = \left[S_0^{-1}(0) + \nu + \frac{f^2}{2c_3 + fc_1}\right]^{-1} \quad (37)$$

displaying a decrease with increasing f. Here $S_0(0) = nc_1$.

Increasing the polymer stiffness, $S_{11}(k)$ of the polyelectrolyte solution decreases further. The position of the maximum k^*l in Figure 1 is readily obtained deriving eq 36,

$$(l/r_0)^4 = [(k^*l)^2 + (\kappa l)^2]^2 \frac{6c_1}{(k^*l)\mathrm{d}(kl)} S_0^{-1}(kl)|_{kl=k^*l} \quad (38)$$

In the approximation:

$$S_0^{-1}(kl) \cong (c_1 n)^{-1}\left(1 + \frac{k^2}{2}\langle R^2{}_G\rangle_p\right) \quad (39)$$

eq 38 becomes[6]

$$[(k^*l)^2 + (\kappa l)^2] = (l/r_0)^2/g(p) \quad (40)$$

Here $g(p)$ is the ratio of the radii of gyration of stiff and Gaussian chains:

$$g(p) = R_G(p)/R_G(0) \approx ((1 + p)/(1 - p))^{1/2} \quad (41)$$

with the last equation valid in the asymptotic limit $n \gg 1$. The maximum of $S_{11}(kl)$, S^*, at k^* is obtained from eq 36 as:

$$S^* = [k^{*2} + \kappa^2]\{[(k^*)^2 + \kappa^2][S_0^{-1}(k^*) + \nu] + \kappa^2(\nu' - \nu)\}^{-1} \quad (42)$$

and introducing the upper approximation for S_0^{-1} and eq 40, it becomes

$$S^* = (l/r_0)^2/g(p)\{[(l/r_0)^2/g(p)][(c_1 n)^{-1} + (k^*l)f^2(p)/12c_1 + \nu] + \kappa^2(\nu' - \nu)\}^{-1} \quad (43)$$

Near θ conditions ($\nu \approx 0$) and in the limit when the electrostatic excluded volume prevails in the denominator of eq 42, we get for large n:

$$S^* = (3/\pi l^2 l_B)^{1/2} f^{-1} c_1^{1/2}[(1 + p)/(1 - p)]^{1/2} \quad (44)$$

For the comparison of calculated k^* and S^* to the static experimental results obtained for gels of PAA, we have chosen here a reference state characterized by these parameters: $c_1 = 0.419$ M, $c_3 = 0$ M, $f = 0.025$, $l_B = 7$ Å, $l = 2.5$ Å, $n = 1000$, and $\nu = 0$.

In Figure 2 the ratio:

$$A = [(k^*l)^2 + (\kappa l)^2]/fc_1^{1/2}l^2 \quad (45)$$

is reported as a function of the stiffness parameter p. For $p = 0$, the Gaussian chain, $A \approx 13$ Å$^{-1/2}$ very far from the experimental value of 2.26 Å$^{-1/2}$. Increasing the stiffness shifts the maximum position k^* toward zero while A decreases reaching values very close to the experimental one. The value $A = 4.6$ Å$^{-1/2}$ predicted by the present theory for $p = 0.8$, the stiffness which in the freely rotating model reproduces the experimental bare persistence length $l_0 = 12$ Å of PAA, is nearer to the observed one than that (8.2 Å$^{-1/2}$) obtained by simple replacement of l^2 by $l_0 l$ in the Gaussian expression[5] for A of eq 40:

$$A = \left(\frac{48\pi l_B}{l^2}\right)^{1/2} \quad (46)$$

The nonzero asymptotic value taken by A near the rod limit is due to a local maximum appearing in the structure factor $S_{11}(k)$ for a small nonzero k^* value. Polymer concentration effects, not shown in this figure, slightly affect A, their influence being greater for high p values. On the other hand, A sensibly increases with the linear charge density at high p, as experimentally observed.[5] Renormalizing the bond length l into $l[(1 + p)/(1 - p)]^{1/2}$ in eq 46 determines a p dependence in A converging to zero in the rod limit. As a consequence, the experimental value is thus recovered at the very high value $p = 0.93$. At much lower p values, the renormalized curve is quite close to the exact FRC result.

The comparison of the theoretical S^* with the experimental value cannot be performed directly as only

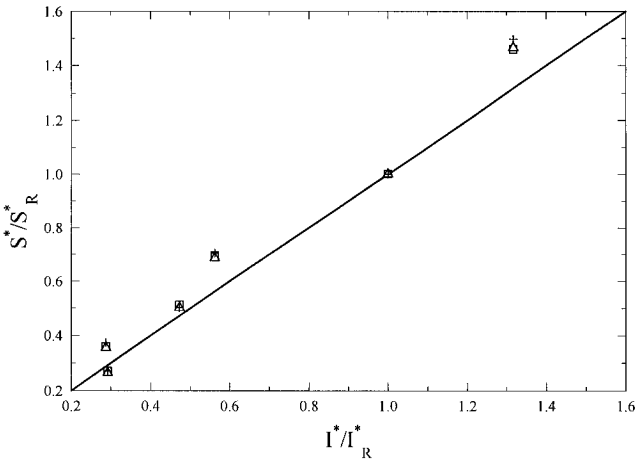

Figure 3. Experimental scattered intensity[5] against theoretical static structure factors normalized to the same reference state (see Figure 2). Symbols (□, △, +) correspond to $p = 0$, 0.5, and 0.8.

values of the scattered intensity I^* proportional to S^* were reported. Therefore we report in Figure 3 the ratios $S^*/\overline{S^*}_R$ plotted against $I^*/\overline{I^*}_R$, where $\overline{S^*}_R$ and $\overline{I^*}_R$ refer to the same reference state. It is interesting to note that changing the stiffness p does not change appreciably the plot showing that S^* is approximately an universal function of p as predicted by eq 44. The experimental points deviate from the theory (represented by the straight diagonal line) only slightly, showing again that eq 44 describes accurately the dependence on concentration and linear charge density.

Dynamic Structure Factor

The dynamic structure factor displays a three-exponential decay with characteristic rate constants $k^2D_G\lambda_a$. The first eigenvalue, $k^2D_G\lambda_1$, describes the relaxation rate of the polymer concentration fluctuations. The second relaxation rate, $k^2D_G\lambda_2$, describes the diffusion of counterions and salt ions to establish a Donnan equilibrium with a diffusion constant:[3]

$$D_G\lambda_2 = \frac{k_B T}{6\pi\eta r} \tag{47}$$

Here r is the Stokes radius of the ions assumed for simplicity equal to $0.25l$. This second eigenvalue is completely unaffected by polymer effects and is much larger than the polymer relaxation rate. The third relaxation rate, $k^2D_G\lambda_3$, is related to the plasmon mode which is driven by electrostatic forces restoring electroneutrality by fast motion of the mobile charges, and it is approximately given, in the $k \to 0$ limit, by the expression:[3]

$$k^2D_G\lambda_3 \cong \kappa^2\frac{k_B T}{6\pi\eta r} = \Lambda_{plasmon} \tag{48}$$

As an illustration, a reference state for the dynamics of concentrated solutions of weakly charged polyelectrolytes is defined by selecting: $c_1 = 1.44$ M, $c_3 = 0$ M, $f = 0.025$, $\nu = 1.445$ M^{-1}, $l_B = 7$ Å, $l = 2.5$ Å, and $n = 1000$, parameters characterizing the PAA system discussed above.

In Figure 4 the ratio $k^2D_G\lambda_3(k)/\Lambda_{plasmon}$ is reported. In the limit $k \to 0$, $k^2D_G\lambda_3(0)$ differs very little from $\Lambda_{plasmon}$: 1% in the reference state, 3.9% at $c_3 = 0.01$, and 8.8% at $f = 0.05$. Stiffness also has a small effect (in the $k \to 0$ limit): 13.7% at $p = 0$. In the $k \to \infty$ limit, $k^2D_G\lambda_3(k)$ becomes linear in k^2 with a diffusion constant uniformly equal to the Donnan constant.

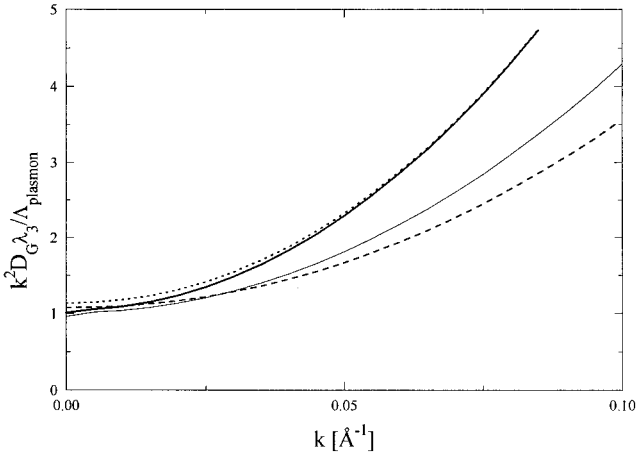

Figure 4. Ratio $k^2D_G\lambda_3(k)/\Lambda_{plasmon}$ as a function of the wavevector k in the dynamic reference state ($l_b = 7$ Å, $l = 2.5$ Å, $c_1 = 1.44$ M, $c_3 = 0$ M, $f = 0.025$, $\nu = 1.445$ M^{-1}, $n = 10^3$): bold curve, $p = 0.8$; dotted curve, $p = 0$; dashed curve, $p = 0.8$, $c_3 = 0.01$; thin curve, $p = 0.8$, $f = 0.05$.

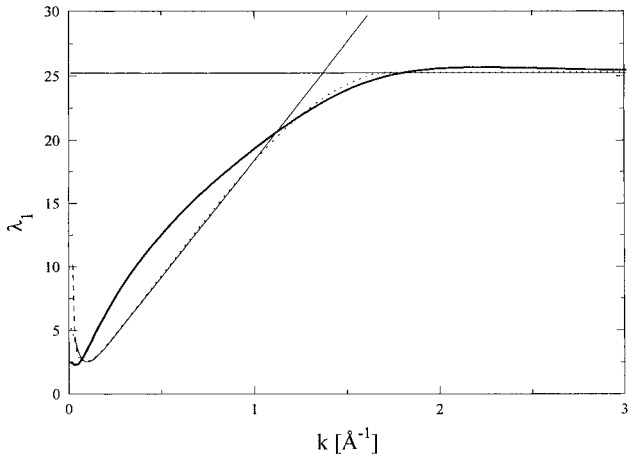

Figure 5. Adimensional polymer eigenvalue, $\lambda_1(k)$, in the reference state: bold curve, $p = 0.8$; dotted curve, $p = 0$. The approximation $\lambda_1{}^a(k)$ of eq 28 in the Gaussian limit: thin curve. The approximation F_{11}, $p = 0.8$: dashed curve. Donnan mode: horizontal straight line.

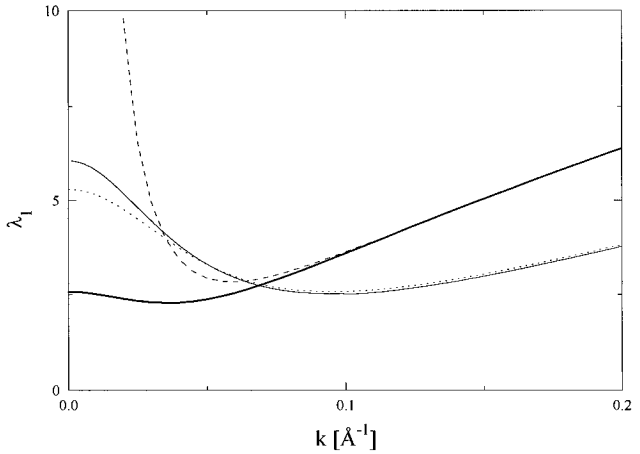

Figure 6. Magnification of $\lambda_1(k)$ of Figure 5 in the small k range.

In Figures 5 and 6 the polymer eigenvalue λ_1 and its approximations, F_{11} and $\lambda_1{}^a$, of eqs 27 and 28 are reported in the large and small k range, respectively. For $kl < 2.5$, the exact result differs very little from $\lambda_1{}^a$, the main difference being in the $k \to 0$ limit where it is

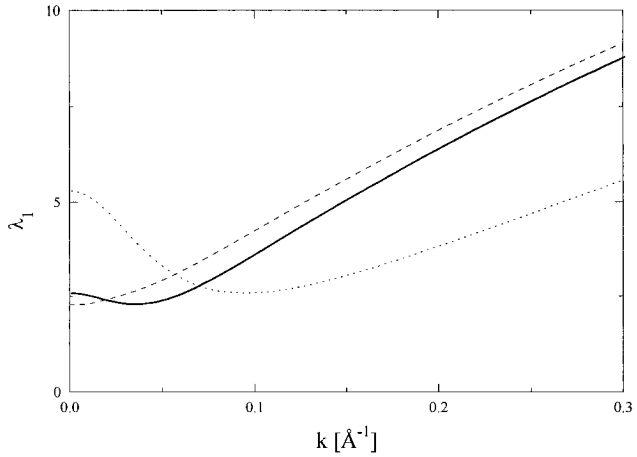

Figure 7. Stiffness effect on the adimensional polymer eigenvalue, $\lambda_1(k)$, in the reference state: dotted curve, $p = 0$; full curve, $p = 0.8$; dashed curve, $p = 0.95$.

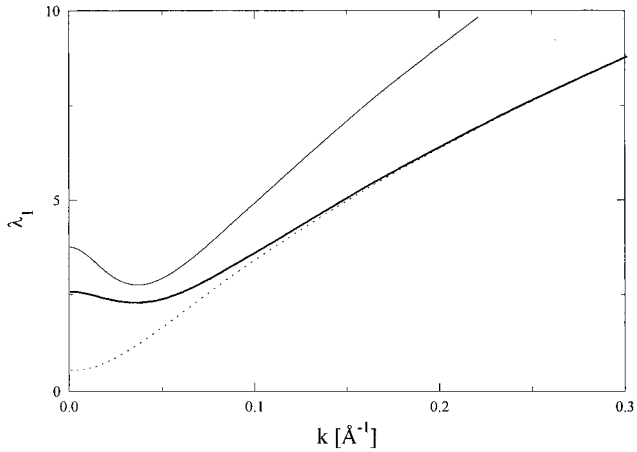

Figure 8. Charge fraction and polymer concentration effects on the polymer eigenvalue, $\lambda_1(k)$, at $p = 0.8$: reference state, bold curve; neutral polymer, dotted curve; $c_1 = 0.707$ M, thin curve.

14% lower. In the intermediate kl range, λ_1 and $\lambda_1{}^a$ are almost coincident and linear in kl (the full rate is here dependent on $(kl)^3$). In the $k \rightarrow \infty$ limit, the exact λ_1 asymptotically converges to the Donnan diffusion coefficient (segments and ions are assumed to have the same friction coefficient), while the approximate $\lambda_1{}^a$ persists in the linear behavior. It is interesting to note that λ_1 is also well approximated by the first diagonal element of the matrix **F** with the exception of the small k range where F_{11} diverges in the $k \rightarrow 0$ limit due to the Coulombic interaction. The appearance of a minimum in λ_1 is a typical effect of the charges, as it is the appearance of a maximum in the static structure factor. The position of the minimum follows eq 38 and is approximately equal to the position of the maximum in $S_{11}(k)$ (as can be appreciated observing that $S_{11}(k)$ sits in the denominator of $\lambda_1{}^a$ of eq 28.

In Figure 7 the behavior of the polymer eigenvalue λ_1 in the small k range as a function of the polymer stiffness in the reference solution is described. It is shown that, increasing stiffness, the position of the minimum of the eigenvalue λ_1 shifts toward lower values while the maximum in $k = 0$ becomes less pronounced. In Figure 8 the effect of charge fraction is described. This effect is relevant only in the small k range, all the curves merging to the neutral behavior at higher k values.

Finally, in Figure 9 the polymer cooperative diffusion coefficient, D_C, of eq 19 is reported against the charge

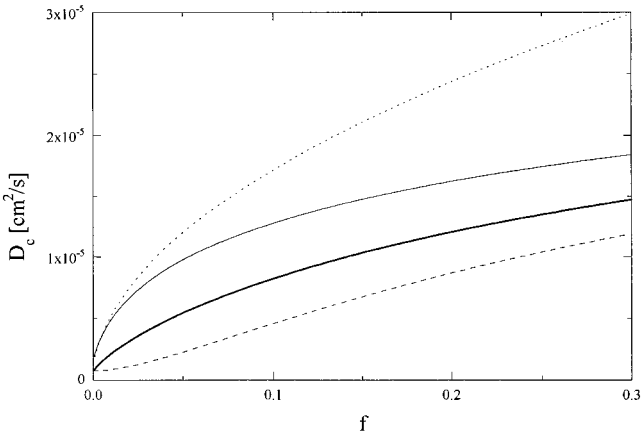

Figure 9. Theoretical cooperative diffusion coefficient of eq 19 as a function of the charge fraction in the dynamic reference state: bold curve, $p = 0.8$; thin curve, $p = 0$; dotted curve, approximation $\lambda_1{}^a(0)$ of eq 28 with Gaussian S_0; dashed curve, the effect of adding salt ($c_3 = 0.1$ M) to the reference state ($p = 0.8$).

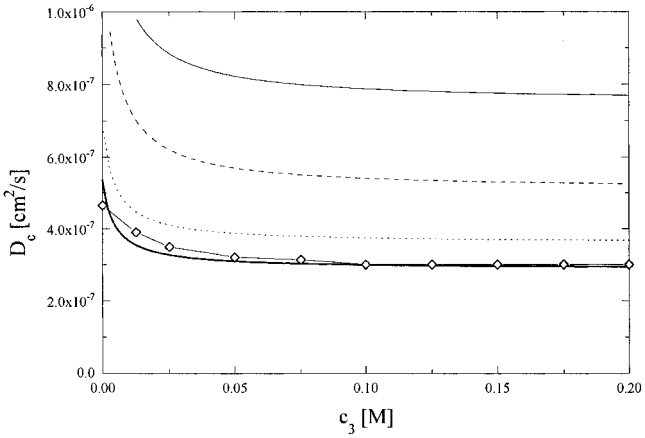

Figure 10. Cooperative diffusion coefficient as a function of salt concentration for PAA, $l_b = 7$ Å, $l = 2.5$ Å, $c_1 = 1.44$ M, $f = 0.006$, $\nu = 1.445$ M^{-1}, $n = 10^3$. Theoretical curves from eq 19: thin curve, $p = 0.8$, $l = 2.5$ Å; dashed curve, $p = 0.989$ (see eq A7 and the discussion therein), $l = 2.5$ Å; dotted curve, $p = 0$, $l = 12$ Å; bold curve, $p = 0$, $l = 15$ Å. Experimental result: ◇.

fraction: Higher curves are obtained for lower polymer stiffness. Note also that the approximate $\lambda_1{}^a$ for flexible polymers is lower than λ_1 at small f but increasingly larger than λ_1 at higher f, and in addition it is much larger than λ_1 for stiff polymers in all the f range. Adding salt results in an overall depression of the curves, while the curvatures also change.

Figure 10 compares the theoretical cooperative diffusion coefficient calculated with the proper choice of parameters with the experimental results obtained by Schoesseler et al.[5] as a function of salt concentration. The virtual bond length parameter, l, has been assumed equal to the vector sum of the two bonds in the monomeric unit of PAA. An increase in the stiffness parameter, p, to values larger than that describing the experimental bare persistence length shifts the theoretical curves toward lower values, thus producing better agreement between theory and experiment. There is a motivation for the use of a larger stiffness based on the electrostatic contribution to the persistence length. An estimation of this effect for flexible polymers is given by eqs A6 and A7 in the Appendix. Even better results are obtained increasing the virtual bond length, l, and balancing p in order to keep the bare persistence length, l_0, constant with the experimental value. The difficul-

ties in the FRC model to describe the cooperative diffusion coefficient, noticeably at low salt concentrations, may suggest that the dynamics in the small k range are sensitive to detailed nearest-neighbor correlations requiring an accurate evaluation of the characteristic ratios. At higher linear charge densities and lower salt concentrations, the agreement between the present theory and the experimental D_C gets worse; this is consistent with the limits of validity of the theory. Using the approximate $D_G\lambda_1^a(0)$ for bond-renormalized flexible chains, a good agreement was found at low salt concentration and high charge density.[6] On the contrary, increasing the salt concentration and decreasing the charge fraction resulted in disagreement: This is somewhat misleading because it is expected that the theory should work better in the latter range. Use of the semiflexible chains has partially clarified this point showing in addition the great sensitivity of the cooperative diffusion coefficient to the description of nearest neighbors correlations.

Conclusions

The static and dynamic structure factors of concentrated solutions of weakly charged polyelectrolytes have been derived in the random phase approximation. Inclusion of the full hydrodynamic interactions and exact solution to the Langevin-linearized dynamical equations enable to derive the effects of stiffness on the full static and dynamic structure factors. The comparison with static and dynamic structure factors measured by SANS on PAA gels shows an interesting capability of the theory of concentrated solutions of semiflexible polymers to explain many of the main features of the experimental behavior. On this basis, we can infer that a more accurate local description of the conformational space of the polymer, by using rotational isomeric state models or accurate empiric force fields to calculate neighbor correlations, should probably improve the agreement of the concentrated solution model to the experimental behavior of gels.

It is to be noted that the model presented here does not take into account the electrostatic effects on the polymer stiffness. These effects can be partially taken into account using the procedures outlined in the Appendix, and for weakly charged polyelectrolytes of modest bare stiffness, a significant increase in the stiffness is expected.

Appendix

If there is an electrostatic effect in the stiffness of the polymer, this will affect the unperturbed dimensions, $\langle R^2_{ij}\rangle$, and in turn the static and dynamic structure factors of the concentrated solution. Describing the vector distance between i and j as the sum of $|i-j|$ bond vectors of the same length l, we can write ($|i-j| > 1$):

$$\langle R^2_{ij}\rangle = l^2|i-j| + 2\sum_{\alpha=1}^{|i-j|-1}[|i-j|-\alpha]\langle\cos(\theta(\alpha))\rangle \qquad \text{(A1)}$$

with $\theta(\alpha)$ the angle between vector $\mathbf{l}_i$ and $\mathbf{l}_{i+\alpha}$. If the polymer is stiff, $\theta(\alpha) \ll 1$,

$$\langle\cos(\theta(\alpha))\rangle \approx 1 - \langle\theta(\alpha)^2\rangle/2, \text{ and}$$

$$\langle R^2_{ij}\rangle = l^2\{|i-j|^2 - \sum_{\alpha=1}^{|i-j|-1}[|i-j|-\alpha]\langle\theta^2(\alpha)\rangle\} \qquad \text{(A2)}$$

Here $\langle\theta^2(\alpha)\rangle$, which is a measure of the polymer curvature, is given,[10] including fluctuations into the Odijk[8,9] derivation of the electrostatic persistence length of the chain configuration, as:

$$\langle\theta^2(\alpha)\rangle = \frac{4}{\pi}\int_0^\infty dq \frac{\sin^2(q\alpha/2)}{q^2}\frac{1}{l_0+\tilde{k}(q)} \qquad \text{(A3)}$$

with

$$\tilde{k}(q) = l_e 2\frac{\kappa^2}{q^2}\left[\left(1+\frac{\kappa^2}{q^2}\right)\ln\left(1+\frac{q^2}{\kappa^2}\right)-1\right] \qquad \text{(A4)}$$

and

$$l_e = l_B/4\kappa^2 f^2 \qquad \text{(A5)}$$

the Odijk electrostatic persistence length and $l_0 = l/(1-p)$ the bare persistence length. Therefore, in the case of a stiff polymer, we could include electrostatic effects on the unperturbed distances (eq A2) and then directly calculate the static and dynamic structure factors of concentrated solutions. It can be immediately recognized that only in the case that l_0 and l_e are large enough, $\langle\theta^2(\alpha)\rangle$ becomes small enough to give meaning to eq A2. In any case the effect predicted by eq A2 is very weak, with the exception of the case $l_0 < l_e$, which is obtained only for strongly charged polyelectrolytes. In the case of PAA, $p = 0.83$, and $f = 0.25$, the polymer is too flexible and weakly charged and eq A2 becomes invalid.

On the opposite limit, when the bare persistence length is small and the polymer flexible, a variational theory[10] gives an electrostatic contribution to the persistence length proportional to the Debye−Huckel screening length:

$$l_p = 5/\kappa \qquad \text{(A6)}$$

This effect can be accounted for in the FRC model by using an increased stiffness parameter, p', corresponding to a persistence length, $l/(1-p')$, derived as the sum of the bare persistence length with l_p:

$$l(1-p')^{-1} = l(1-p)^{-1} + l_p \qquad \text{(A7)}$$

In the PAA experimental conditions, $l_p = 212.2$ Å and $p' = 0.989$.

References and Notes

(1) Doi, M.; Edwards, S. F. *The Theory of Polymer Dynamics*; Clarendon Press: Oxford, 1986.
(2) Perico, A.; Siciliano, A. *Macromolecules* **1995**, *28*, 1709.
(3) Ajdari, A.; Leibler, L.; Joanny, J. F. *J. Chem. Phys.* **1991**, *95*, 4580.
(4) Borue, V.; Erukhimovich, J. *Macromolecules* **1988**, *21*, 3240.
(5) Schoesseler, F.; Ilmain, F.; Candau, S. J. *Macromolecules* **1991**, *24*, 225.
(6) Schoesseler, F.; Moussaid, A.; Munch, J. P.; Candau, S. J. *J. Phys. II (France)* **1991**, *1*, 1197.
(7) Joanny, J. F.; Leibler, L. *J. Phys. (France)* **1990**, *51*, 545.
(8) Odijk, T. *J. Pol. Sci. Pol. Phys. Ed.* **1977**, *15*, 477.
(9) Odijk, T.; Houwaart, A. C. *J. Pol. Sci. Pol. Phys. Ed.* **1977**, *16*, 627.
(10) Barrat, J. L.; Joanny, J. F. *Europhys. Lett.* **1993**, *24*, 333.
(11) Yamakawa, H. *Modern Theory of Polymer Solutions*; Harper and Row: New York, 1971; p 37.

MA9513372